CHAPTER E-7 SEISMIC EVALUATION OF RETAINING

E-7.1 Key Concepts

E-7.1.1 Description of Potential Failure Mode

This potential failure mode typically relates to gated spillway crest structures such as the one shown on Figure E-7-1. If the spillway is not gated, there is less potential for a failure mechanism that results in an uncontrolled release of the reservoir. Also, if the spillway is not gated, the water level will typically be low on the crest structure walls where wall deflections are smaller, thus reducing the possibility of a seepage path on the outside of the walls that the reservoir can access. Spillway crest structures are often located on one of the abutments of an embankment dam, with the embankment abutting against one of the structure sidewalls. As a result, the embankment serves as backfill for the crest structure wall and loads the wall both statically and dynamically. If he wall displaces enough during an earthquake, a seepage path

Figure E-7-1 – Spillway Crest Structure Adjacent to Embankment Dam

between the crest structure wall and the embankment can develop. This potential failure mode can progress in two different ways. If the earth pressure loading results in collapse or at least large deformation of the spillway wall, the spillway gates adjacent to the wall can fail due to loss

of support or loading from the wall deflections. If the gates do not fail from wall deflections, there is the possibility that the deflections will create a seepage path behind the crest structure wall. If the seepage path is low enough that it can be accessed by the reservoir, seepage may erode the embankment materials and ultimately lead to a breach of the embankment dam as shown on the exaggerated illustration provided on Figure E-7-2.

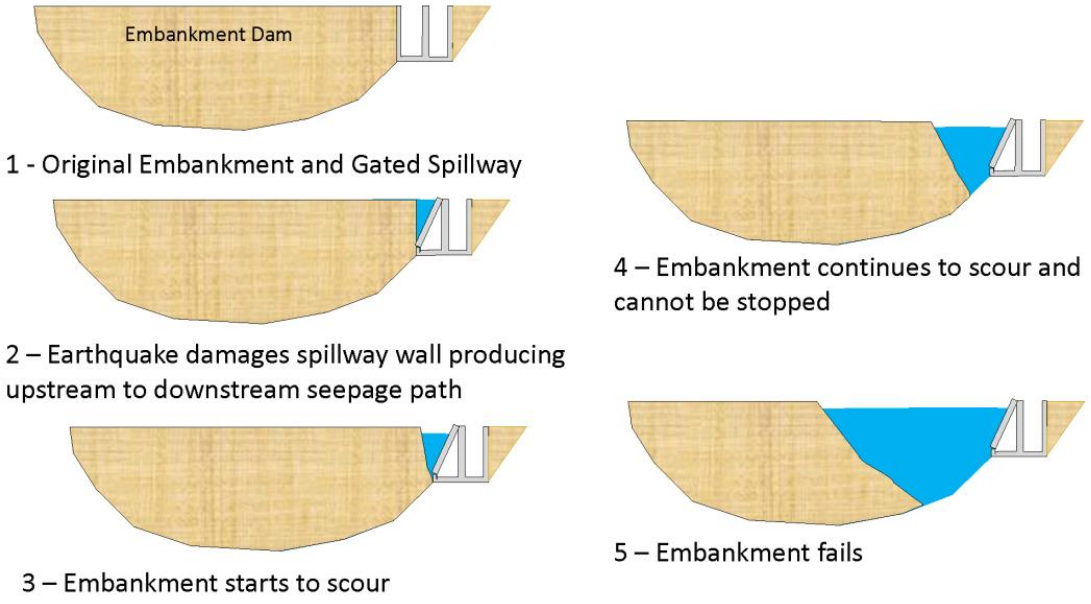

Figure E-7-2 – Embankment Failure Due to Spillway Sidewall Deflection and Subsequent Erosion Behind the Wall

E-7.1.2 Reservoir Water Surface Elevation

Reservoir water level on the spillway walls and gates is a key parameter since it can affect the loading on the walls (both statically and dynamically), the access to a potential seepage path behind the crest structure walls due to wall deflections during an earthquake, and also the consequences of wall failure due to the effect on the breach outflow.

E-7.1.3 Wall Geometry

The wall geometry (height and thickness of the wall) and whether the wall is counterforted will affect how the wall is excited during an earthquake. A stiffer wall may attract more load, while a more flexible wall may relieve load and dissipate energy through deflection. However, a more

flexible wall may also respond more to an earthquake, depending on its natural frequency relative to the frequency content of the earthquake ground motions. Three dimensional studies of spillway crest structures in contact with the abutment of an embankment dam have indicated that seismic earth pressure loads can increase if the dam axis at the crest structure is angled downstream relative to the wall, compared to the case where the axis is normal to the wall.

E-7.1.4 Moment Capacity

The moment capacity of the wall will be a function of the steel reinforcement provided at a given location within the spillway wall. The tensile strength of the concrete can also contribute to the moment capacity, although concrete is generally weak in tension.

E-7.1.5 Shear Capacity

The shear capacity of a wall will, in most cases, consist of the shear capacity of the concrete. For cases where shear reinforcement is provided, the shear capacity will be a combination of the reinforcement shear capacity and the concrete shear capacity. If the concrete cracks due to large tensile stresses during an earthquake, the shear capacity can be reduced but the frictional effects will still be present, and the tendency for dilation of the cracks during shearing can increase the tension in the steel and hence the normal force acting across the cracks (which translates to higher frictional resistance).

E-7.1.6 Seismic Hazard

Most spillway walls will have some reserve capacity beyond the stress levels created by static loads. However, the level of seismic loading in combination with the static loading will determine whether the walls are overstressed and, if so, to what level.

E-7.1.7 Wall Backfill

The properties of the wall backfill will determine the seismic earth pressure against crest structure walls. The saturation level of the backfill will also influence the static and dynamic pressures on the wall, and can be an indication of the ability of water to move through the soil, developing a seepage path along the spillway crest structure walls where internal erosion could initiate.

E-7.1.8 Counterforted Walls

Many spillway crest structure walls, especially those for gated structures, are counterforted. The counterforts are concrete walls that extend into the soil to which the wall panels are attached. Frictional resistance between the soil and counterforts helps keep the wall in place. For wall heights exceeding 40 feet, a counterforted wall is typically provided. A counterforted wall is more complicated to analyze than a cantilever wall. A counterforted wall can fail through a number of mechanisms including moment or shear failure in the counterforts, moment or shear failure in the wall panels between counterforts and failure of connecting steel between the wall panels and the counterforts. The various failure mechanisms are shown in Figure E-7-3.

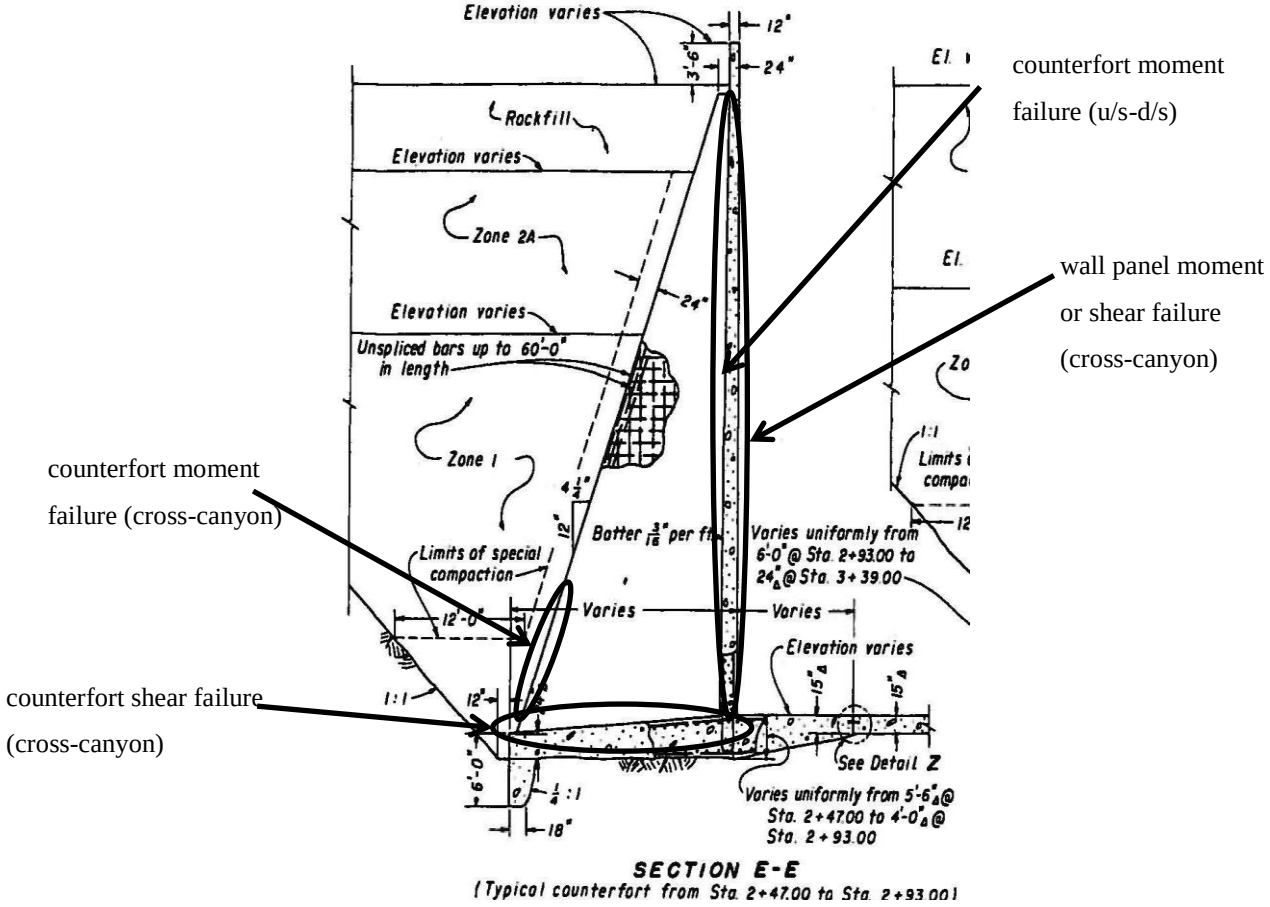

Figure E-7-3 – Failure Mechanisms for Counterforted Walls

E-7.1.9 Seismic Earth Pressure Theories

Seismic soil loadings on walls are typically related to earth pressure theory and the state of the wall backfill prior to and during the earthquake. The Rankine theory of earth pressures for active and passive conditions (1857) can be used to estimate the state of stress within a soil mass that, because of displacement of the wall into (passive) or away from (active) the soil mass, is transformed from an at-rest state to a state of plastic equilibrium. The orientation of the assumed linear failure surface within the soil mass is also determined in the analysis. The shear stress at failure within the soil is defined by a Mohr-Coulomb shear strength relationship.

The Coulomb wedge theory (1776) looks at the equilibrium of forces acting on a soil wedge, without considering the state of stress in the soil. The wedge theory assumes a linear slip plane within the backfill and full mobilization of the shear strength along this failure surface. Interface friction between the wall and the backfill may be considered in the analysis.

In addition to the theories described above, numerous authors have developed relationships for active and passive earth pressure, based on the assumption of a logarithmic failure surface. Rankine's theory, Coulomb's wedge theory, and the logarithmic spiral procedure result in similar values for active and passive earth pressure when the friction angle between the backfill and the wall surface is assumed to be zero. For interface friction angles greater than zero, the wedge method and the logarithmic spiral procedure result in nearly the same value for active earth pressures. The logarithmic spiral procedure results in reasonably accurate values for passive earth pressures, for all values of the friction angles between the wall and the backfill. The accuracy of the passive earth pressure computed by the wedge method diminishes with increasing values of wall/backfill friction, due to the fact that the boundary of the failure block becomes increasingly curved.

Okabe (1926) and Mononobe and Matsuo (1929) built on Coulomb's theory of active and passive earth pressure to include the effects of dynamic earth pressures on walls. Specifically, the pioneering work for dynamic soil-structure interaction was performed in Japan following the Great Kwanto Earthquake of 1923 by Okabe and Mononobe and Matsuo. The method proposed by these researchers is known as the Mononobe-Okabe method and, along with its derivatives,

has generally been considered the most commonly used approach to determine seismically induced lateral earth pressures. The M-O method is based on Coulomb's wedge theory of static lateral earth pressures and was originally developed for gravity walls retaining cohesionless backfill materials.

A significant aspect to development of the widely-accepted Mononobe-Okabe method was the first known physical experiments performed for the purpose of investigation seismic earth pressure on retaining walls by Mononobe and Matsuo in Japan. The experiment was performed using a rigid small-scale 1g shake table. The 9-foot long by 4-foot wide by 4-foot or 6-foot high sand boxes that contained the relatively loose and dry sands were set on rollers as shown on Figure E-7-4. A winch driven by a 30 horsepower electric motor was used to provide the horizontal simple harmonic motion of the shake table, and the hydraulic pressure gauges at the top of the sand boxes measured the resulting seismic earth pressures.

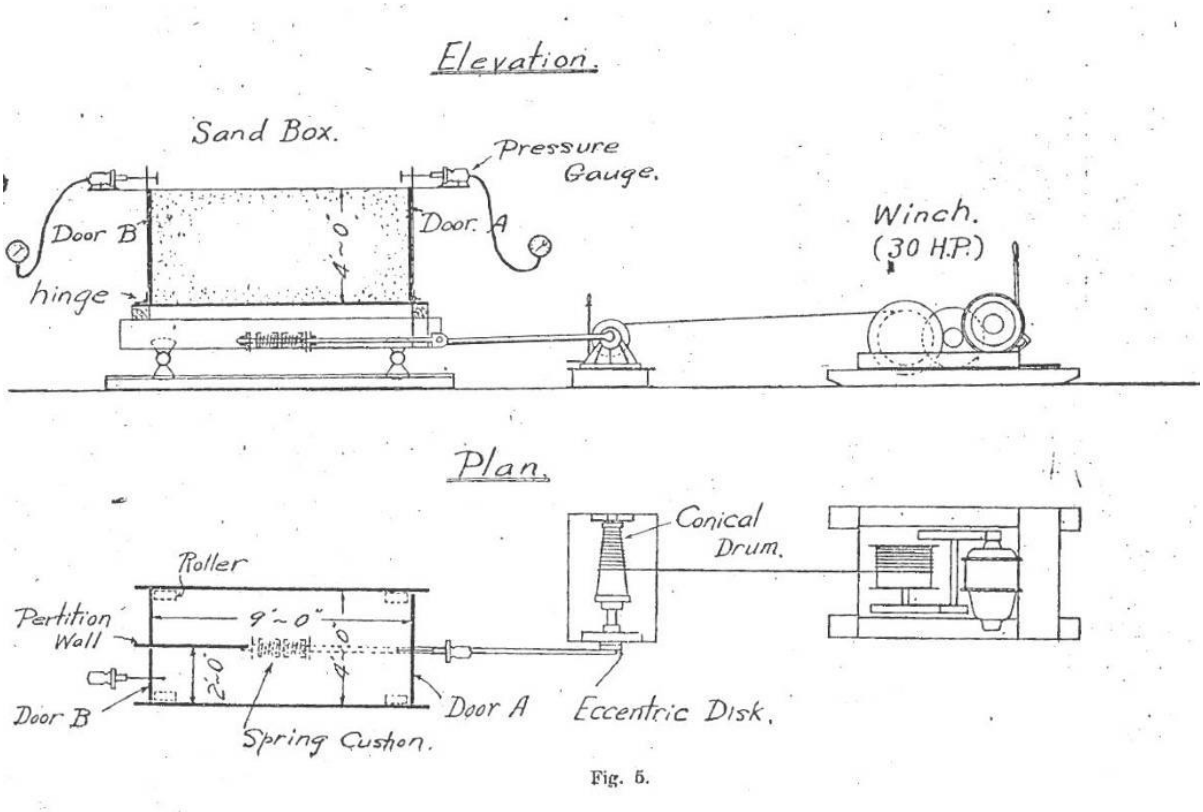

Figure E-7-4 – Setup of Mononobe and Matsuo Experiments

The Mononobe-Okabe theory includes the effects of earthquakes through the use of constant horizontal acceleration and constant vertical acceleration, which is expressed as a fraction of the acceleration of gravity (1.0 g = 32.174 ft/sec/sec). The acceleration values act on the soil mass comprising Coulomb's active or passive wedge. The Mononobe-Okabe theory assumes that wall movements are sufficient to fully mobilize the shear resistance along the backfill wedge failure surface, which is consistent with the Coulomb theory. For dynamic active earth pressures (dynamic active earth pressure force, P_{AE}), the wall movements are away from the backfill and for dynamic passive earth pressures (dynamic passive earth pressure force, P_{PE}), the wall movements are towards the backfill. The Mononobe-Okabe theory gives the net static and dynamic force. For positive horizontal accelerations (soil accelerates toward the wall), the net dynamic active force is greater than the net static active force and the net dynamic passive force is less than net static passive force (Ebeling and Morrison, 1992). For both static and dynamic earth pressures, wall movements are required to reach the minimum active and maximum passive earth pressure conditions. Table E-7-1 shows relative displacements needed to mobilize these pressures, where Y is the movement of the top of the wall due to tilting or lateral translation and H is the height of the wall (Clough and Duncan, 1991). Typically, it is assumed that the wall moves away from the soil, and active pressures are developed. Passive pressures would be unusual requiring a mechanism that would move the wall into the soil. However, finite element model results for spillways located adjacent to rock abutments with dam embankments abutting against the other side of the structure have demonstrated that such a mechanism can develop. If the wall is rigid and the predicted displacements are less than those indicated in Table E-7-1, at rest earth pressures will likely develop. The Mononobe-Okabe theory does not include the effect of saturation of the soil, as the static Coulomb and Rankine approaches can.

Table E-7-1 – Wall Movements Needed to develop Pressures

Type of Backfill	Values of Y/H*	
	Active	Passive
Dense Sand	0.001	0.01
Medium-Dense Sand	0.002	0.02
Loose Sand	0.004	0.04

* Y = horizontal displacement at top of wall; H = height of wall

Wood evaluated dynamic earth pressures for walls retaining non-yielding backfill, assuming elastic material (Wood, 1973). Wood provided normal mode solutions for the case of both a uniform modulus and a modulus varying with depth. Since these solutions are slowly convergent for practical problems, Wood presented approximate procedures based on findings from the normal mode solutions. The normal stress distributions along the back of the wall were found to be related to Poisson's ratio and the lateral extent of the backfill behind the wall. Figure E-7-5 presents Wood's formulation for the case of a uniform horizontal body force. It should be noted that Wood's method assumes a rigid wall and therefore small displacements and may not be suitable for evaluating a failure condition. However, it can be a useful tool in screening-level risk assessment for sites with high peak horizontal accelerations.

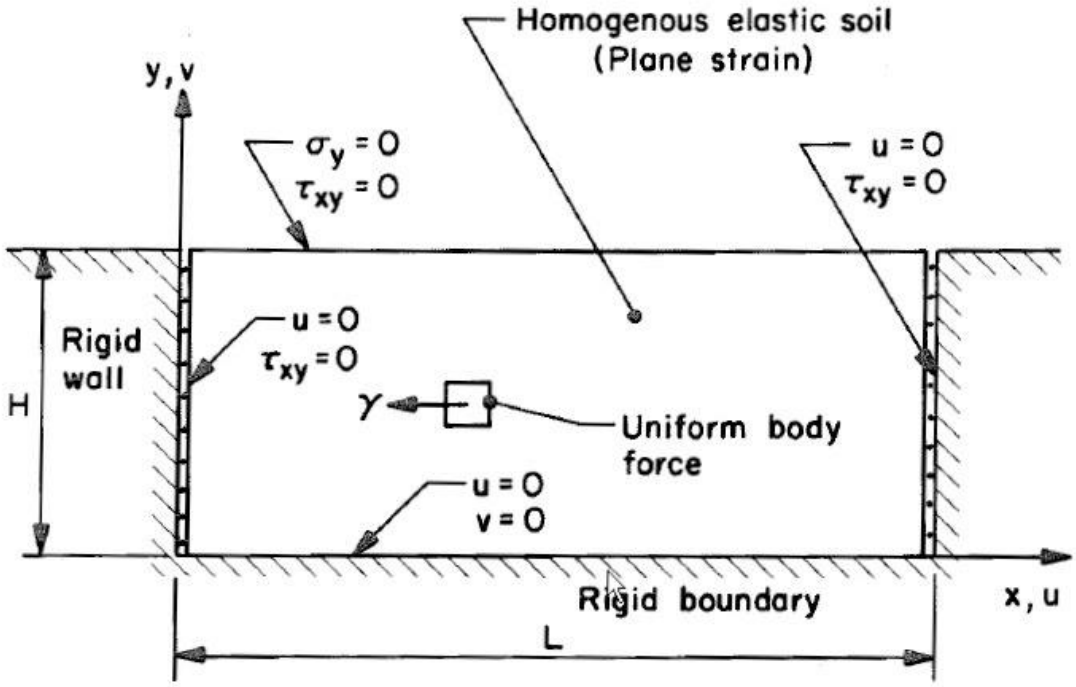

Figure E-7-5 - Woods Rigid Problem

Other methods for evaluation of dynamic soil-structure interaction problems have been developed more recently by Ostadan and White (1997) and Maleki and Mahjoubi (2010). Specifically, the Ostadan and White method is for non-yielding walls and fully considers the frequency content of the earthquake for developing seismic earth pressure loads. The Maleki and Mahjoubi method includes approaches for both yielding and non-yielding walls and is focused on the natural period of the soil-wall system. Comparisons of these various methods are often completed for evaluation of gated spillway sidewalls subjected to earthquake loads significantly greater than those used to originally design the structure. An example of such a comparison is shown in Figure E-7-6. Equations 11, 12 and 13 of the Maleki and Mahjoubi (2010) method calculate the maximum seismic soil pressure based on either the peak ground accelerations (Eq 11), area under the pseudo acceleration response spectrum (Eq 12) or the peak spectral acceleration (Eq 13) and result in similar pressures as shown below.

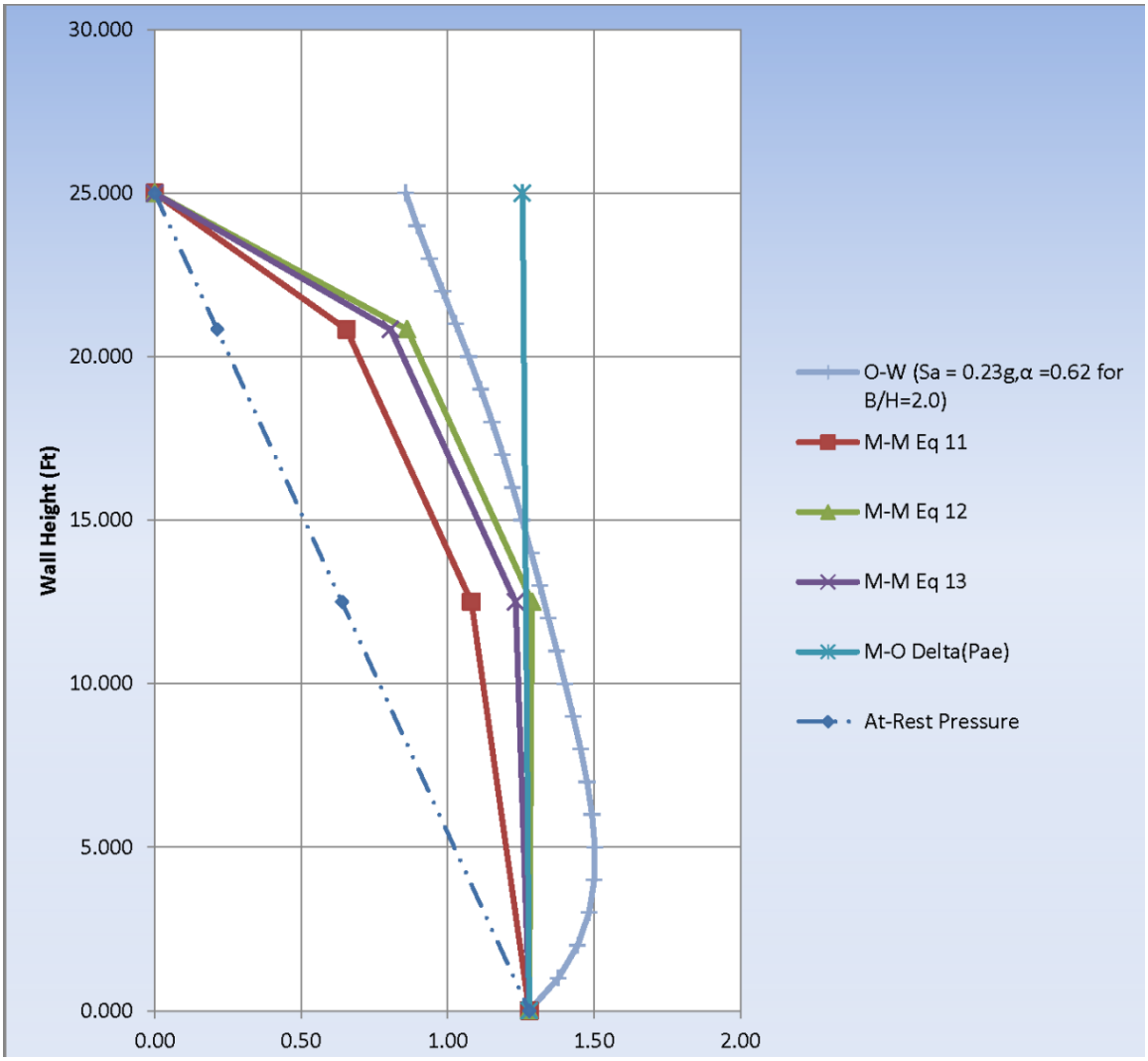

Figure E-7-6 – Total Seismic Lateral Earth Pressure (kips/ft^2) Comparison Based on the Summation of At-Rest and Seismic Increment

E-7.1.10 Screening

This potential failure mode generally only applies to spillways that are gated. If the spillway is not gated, it is unlikely that there will be an uncontrolled release as a result of wall failure (the exception would be a wall where deflections could create a seepage path behind the wall that the reservoir could access). Finally, if a simple pseudo-static analysis indicates that applied loads result in moment and shear stresses that are within the capacity of the wall and there are no other

issues associated with the anchorage of the gates or deflections of the wall, this potential failure mode can be classified as being remote.

E-7.2 Determination of Static and Seismic Earth Pressures

For soil backfill that is cohesionless and dry, the horizontal effective stress (σ) at any depth due to static earth pressures is obtained from:

$$\sigma = K\gamma Z \qquad \textbf{Equation E-7-1}$$

where: K is either the active (K_A), passive (K_P), or at rest (K_O) earth pressure coefficient

γ = the unit weight of the soil backfill

Z = depth of backfill at the desired location along the wall

The resultant horizontal static earth force is equal to:

$$P = K \tfrac{1}{2} \gamma H^2 \qquad \textbf{Equation E-7-2}$$

where: H = the full depth of the backfill acting on the wall

The total earth pressure acting on a wall with a portion of the backfill saturated is composed of several components, including: the drained unit weight of the soil above the water level; the buoyant weight of the soil below the water level; and, the hydrostatic pressure of the water. The resultant force acts along the back of the wall at one-third H above the heel of the wall. Active and passive static earth pressures can be estimated using the Coulomb theory. The key parameters needed to determine active and passive earth pressure coefficients are shown in Figure E-7-7 (Ebeling and Morrison, 1992).

The active earth pressure coefficient is provided by:

$$K_A = \frac{\cos^2(\phi - \theta)}{\cos^2\theta \cos(\theta + \delta)\left[1 + \sqrt{\frac{\sin(\phi + \delta)\sin(\phi - \beta)}{\cos(\delta + \theta)\cos(\beta - \theta)}}\right]^2}$$

Equation E-7-3

The passive earth pressure coefficient is provided by:

$$K_P = \frac{\cos^2(\phi + \theta)}{\cos^2\theta \cos(\delta - \theta)\left[1 - \sqrt{\frac{\sin(\phi + \delta)\sin(\phi + \beta)}{\cos(\delta - \theta)\cos(\beta - \theta)}}\right]^2}$$

Equation E-7-4

Earth pressures greater than those predicted by the above equations can be exceeded if the fill is compacted tightly against the wall (Duncan, Williams, Sehn, and Seed, 1991).

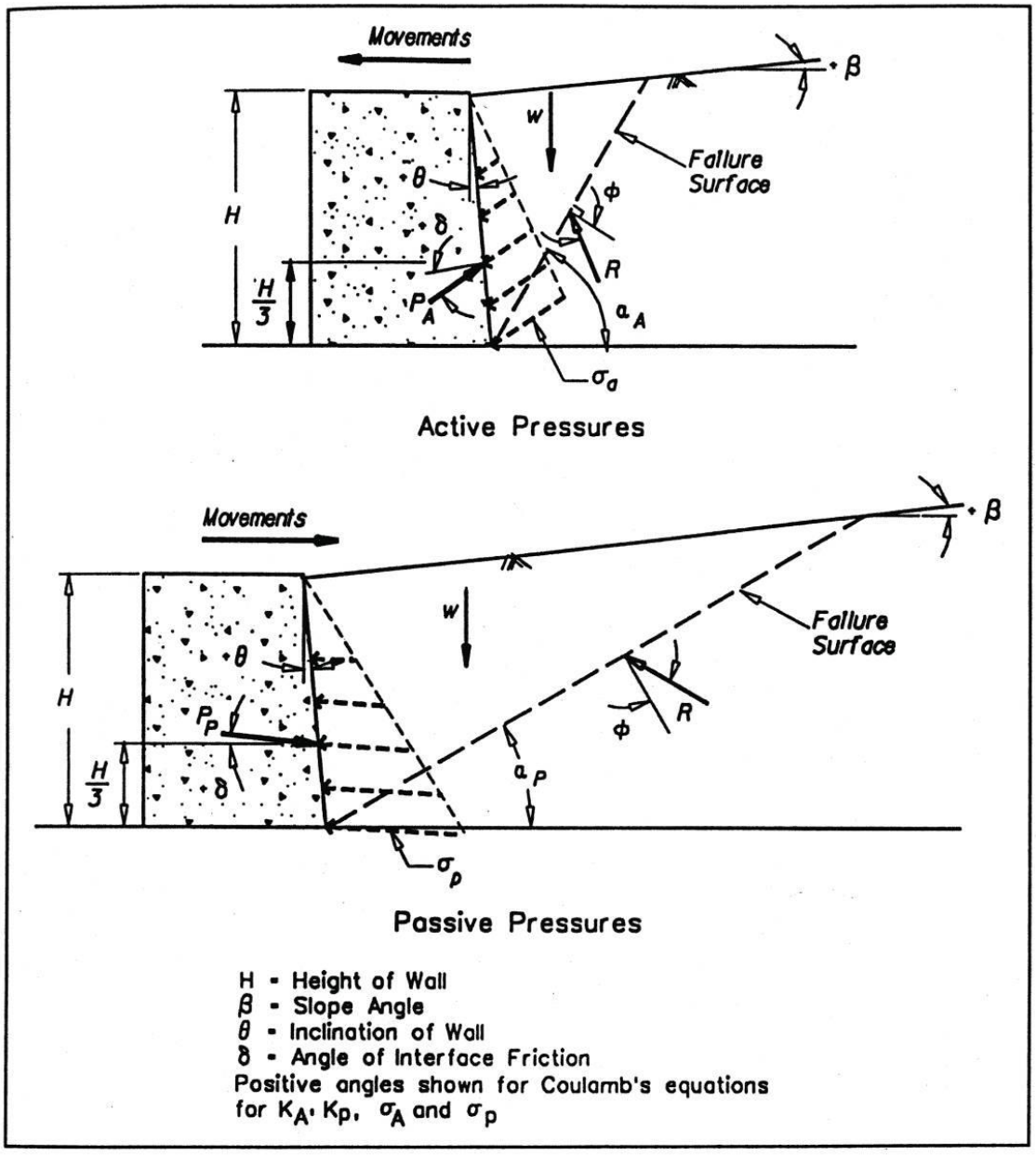

Figure E-7-7 Coulomb Active and Passive Earth Pressures (from Ebeling and Morrison, 1992)

If at-rest static earth pressures develop, the at-rest earth pressure coefficient can be estimated by the following equation for normally consolidated soils:

$K_O = 1 - \sin \varphi$ **Equation E-7-4**

For overconsolidated soils and compacted soils, the value of K_O can be larger than that provided by the above equation and can be as high as 2.0 (Wu, 1975).

There are a variety of approaches that can be used to estimate the dynamic earth pressure on a wall during an earthquake.

E-7.2.1 Mononobe-Okabe

The Mononobe-Okabe relationship provides the total earth pressure load as a result of earthquake loading on a somewhat flexible wall, behind which the backfill has yielded. The Mononobe-Okabe relationship for the resultant active earth force, P_{AE}, based on Whitman and Christian (1990) can be expressed as follows:

$P_{AE} = K_{AE}[1/2(\gamma_t(1 - k_v))H^2]$ **Equation E-7-5**

The dynamic active earth pressure coefficient is given by:

$$K_{AE} = \frac{\cos^2(\phi - \psi - \theta)}{\cos\psi\cos^2\theta \cos(\psi + \theta + \delta)\left[1 + \sqrt{\frac{\sin(\phi + \delta)\sin(\phi - \psi - \beta)}{\cos(\delta + \psi + \theta)\cos(\beta - \theta)}}\right]^2}$$

Equation E-7-6

In this equation, ψ is the seismic inertia angle, which is defined as:

$\psi = \tan^{-1}(k_h/(1- k_v))$ **Equation E-7-7**

where k_h and k_v are the horizontal and vertical seismic coefficients.

The active earth force represents the total static and dynamic earth force and acts at an angle δ from the normal to the back of the wall. A limited number of model tests performed by Sherif and Fang (1983) and Matsuzawa, Ishibashi and Kawamura (1985) on dry sands indicated that δ

ranges from φ/2 to 2φ/3. Figures E-7-8 and E-7-9 provide values of K_{AE}, based on a number of parameters. The Mononobe-Okabe analysis procedure does not identify the location of the resultant earth pressure force along the height of the wall. Analytical studies and physical models have indicated that the resultant force acts at a location that ranges from 0.4 to 0.55 times the height of the wall, measured from the base of the wall. The vertical component of the resultant force depends on the magnitude of the accelerations applied to the mass comprising the soil wedge.

The effects of saturated backfill need to be considered and will be a function of whether pore water pressures increase within the backfill during an earthquake and the whether the water in the backfill is restrained or free, which is a function of the permeability of the backfill (Ebeling and Morrison, 1992).

The Mononobe-Okabe relationship for the resultant passive earth force, P_{PE}, based on Whitman and Christian (1990) can be expressed as follows:

$$P_{PE} = K_{PE}[1/2(\gamma_t(1 - k_v))H^2] \qquad \textbf{Equation E-7-8}$$

The dynamic passive earth pressure coefficient is given by:

$$K_{PE} = \frac{\cos^2(\phi - \psi + \theta)}{\cos\psi \cos^2\theta \cos(\psi - \theta + \delta)\left[1 - \sqrt{\frac{\sin(\phi + \delta)\sin(\phi - \psi + \beta)}{\cos(\delta + \psi - \theta)\cos(\beta - \theta)}}\right]^2}$$

Equation E-7-9

In this equation, ψ is the seismic inertia angle, which is defined above.

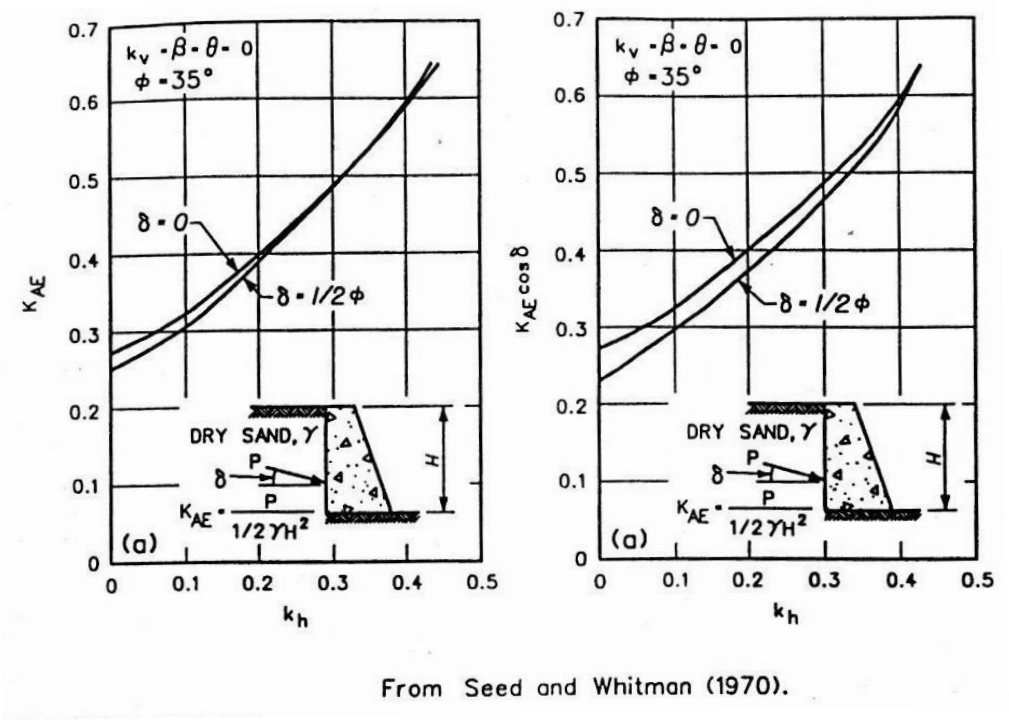

Figure E-7-8 – Values of K_{AE} (from Ebeling and Morrison, 1992)

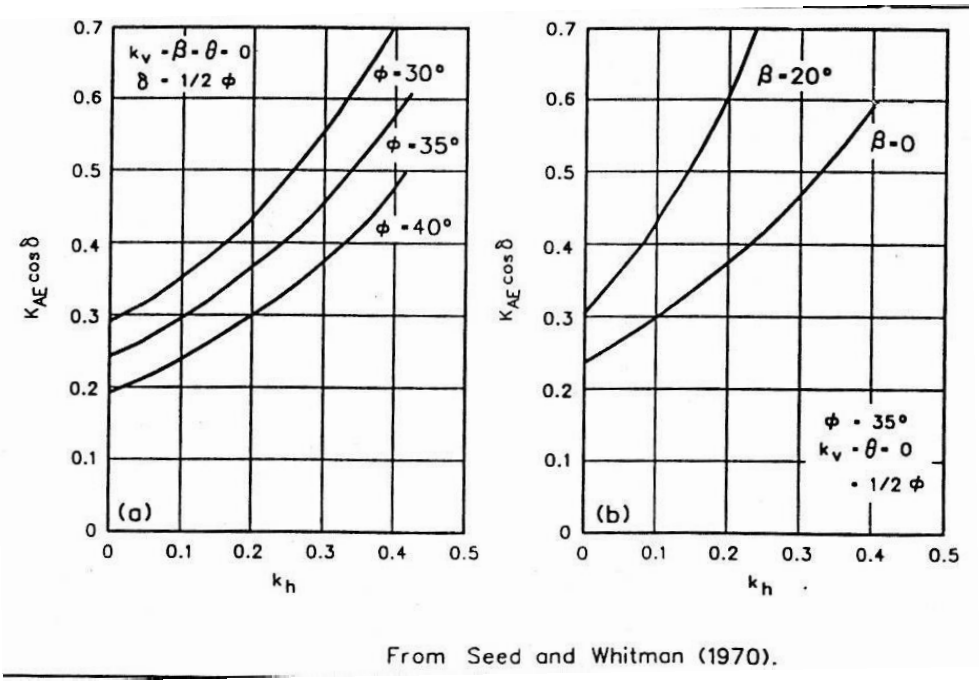

Figure E-7-9 – Values of K_{AE} (from Ebeling and Morrison, 1992)

In 1970, Seed and Whitman completed parametric studies on δ, φ and β and were the first to introduce the concept of an incremental dynamic earth pressure component that when added to the active (driving wedge) or passive (resisting wedge) lateral earth pressure resulted in the same total dynamic force acting on the wall as that predicted by the Mononobe-Okabe method. Seed and Whitman proposed that the incremental dynamic component was an inverted triangular pressure distribution with a force resultant that acted at 2/3H from the base of the wall as shown in Figure E-7-10.

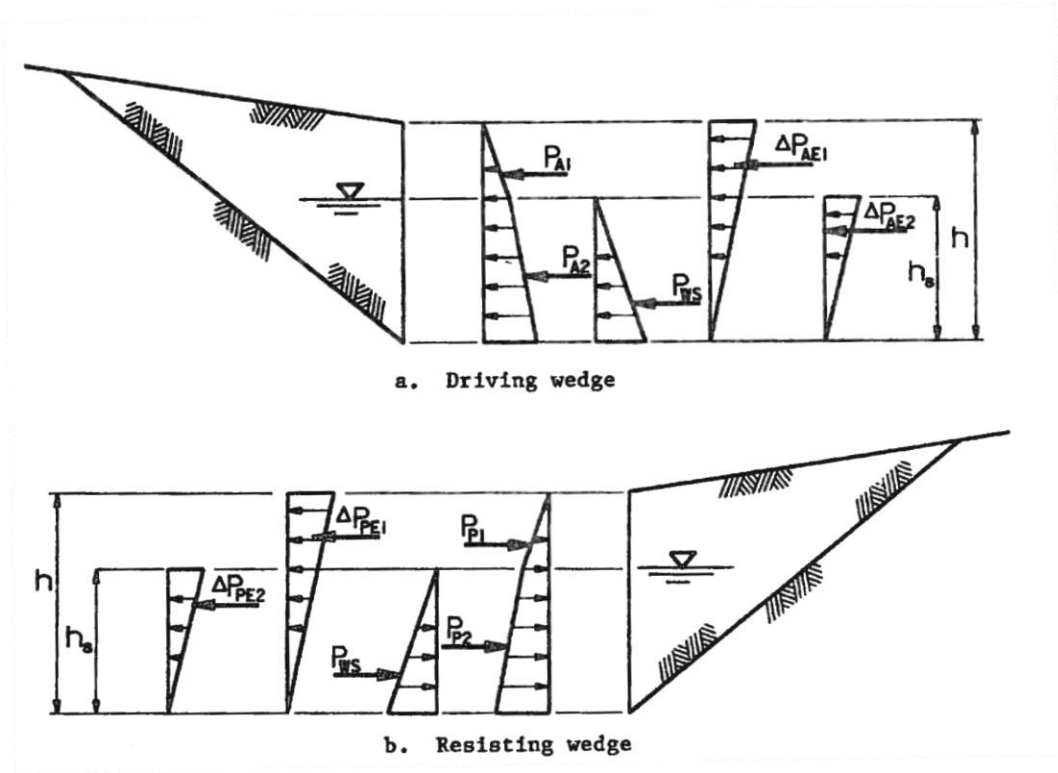

Figure E-7-10 – Total Seismic Lateral Earth Pressures Consisting of Active/Passive Components and Increment Dynamic Components (from Seed and Whitman, 1970)

It should be noted that, as the horizontal seismic coefficient, k_h, increases, the angle of the failure surface, α_a, decreases, until eventually it becomes equal to β, making the sliding wedge infinite, which makes the calculated force on the wall infinite. Numerically, this occurs when the seismic inertia angle, ψ, is greater than the angle of internal friction of the soil, φ. Beyond this point, the calculated force becomes undefined, due to a negative number appearing inside a square root

sign in the denominator. When that point is reached, the calculated value of K_{AE} or K_{PE} becomes infinite, producing earth pressures that are physically impossible. This is only an issue with very high horizontal accelerations, but many dams are located in high seismic areas where such loadings are possible.

E-7.2.2 Wood's Solution

Wood's solution provides an estimate of dynamic earth pressures for rigid walls with non-yielding backfill (Wood, 1973). The dynamic earth pressures obtained from this method must be added to the static earth pressures to obtain the total earth pressures during an earthquake. Because the wall is assumed rigid, the static earth pressure component is assumed to be at-rest earth pressure. Figure E-7-11 presents two examples of the variation in the values for normalized horizontal stresses with normalized elevations above the base of a wall, based on Wood's solution (Wood, 1973). An L/H value of 1 (where L = the width of backfill and H = the wall height) corresponds to a narrow backfill placed within rigid containment and an L/H value of 10 represents a backfill of great width. The horizontal stresses (σ_x) at any vertical location Y, along the wall, are normalized by the product of γH in Figure E-7-11. Figure E-7-12 provides the corresponding resultant horizontal force, F_{sr}, and the corresponding seismic moment about the base of a rigid wall, M_{sr}, as a function of Poisson's ratio, ν, and L/H. The height at which the resultant force acts on the wall can be determined by computing $Y_{sr} = M_{sr}/F_{sr}$. The stresses shown in Figure E-7-11 and the moments and forces shown in Figure E-7-12 are based on a 1.0g horizontal acceleration. For other horizontal accelerations, the values from Figures E-7-11 and E-7-12 can be factored by the horizontal acceleration value expressed as a fraction of gravity (for a horizontal acceleration of 0.5 g, the stresses, moments and shear values should be multiplied by 0.5). Shake table tests by Yong (1985), confirmed the applicability of Wood's solution when the predominant frequency of shaking is significantly less than the fundamental frequency of the backfill. The measured forces exceeded the forces predicted by the Mononobe-Okabe theory by a factor of 2 or 3, except at very large accelerations, where Mononobe-Okabe "blows up."

It should be noted that accelerations at the base of the wall should be used in the simplified methods described above. If the wall is founded on soil and the seismologists provide bedrock

accelerations at some depth below the base of the wall, then the accelerations must propagate up through the soil and could be considerably different than the bedrock accelerations. Programs such as SHAKE can be used to propagate the motions and estimate the accelerations at the base of the wall. The tests by Yong showed that if the ground accelerations are magnified up through the backfill, much greater earth pressures can result than those predicted by using the accelerations at the base of the wall. Therefore, in these cases it may be appropriate to use accelerations at 1/3 to 1/2 the height of the wall above the base as determined by a SHAKE analysis or similar.

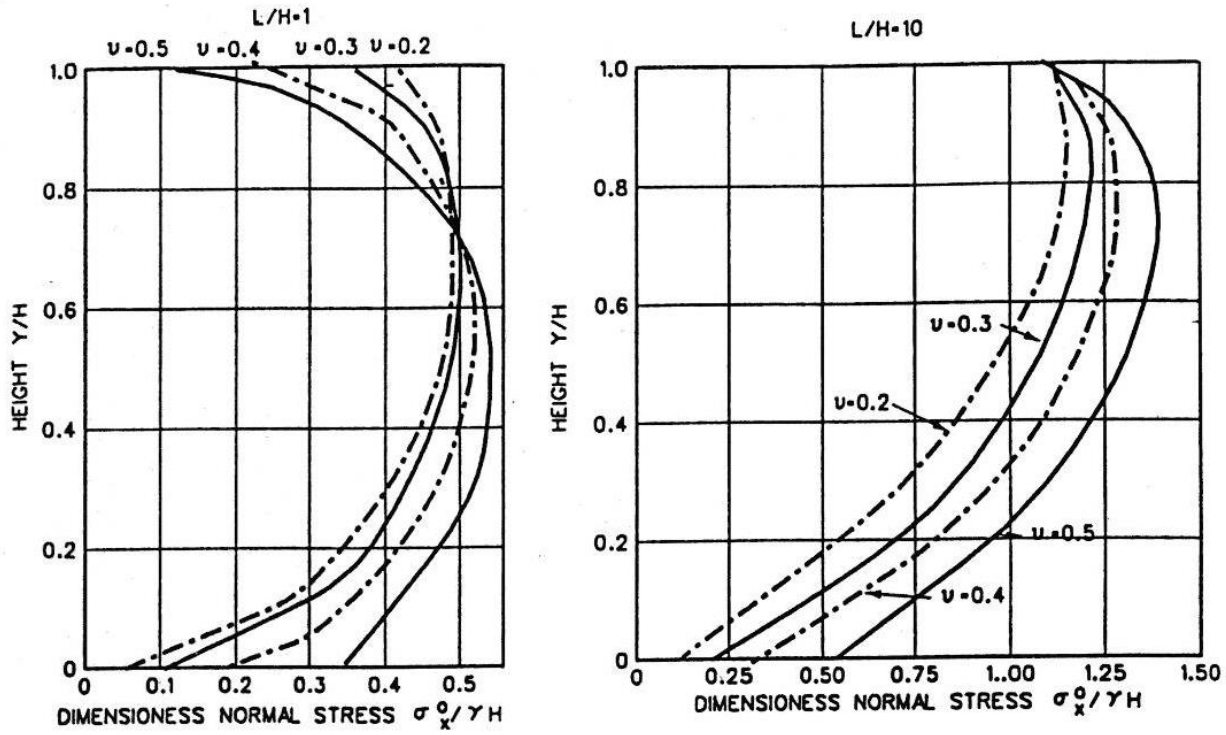

Figure E-7-11 – Normal Wall Stresses from Wood's Solution (from Ebeling and Morrison, 1992)

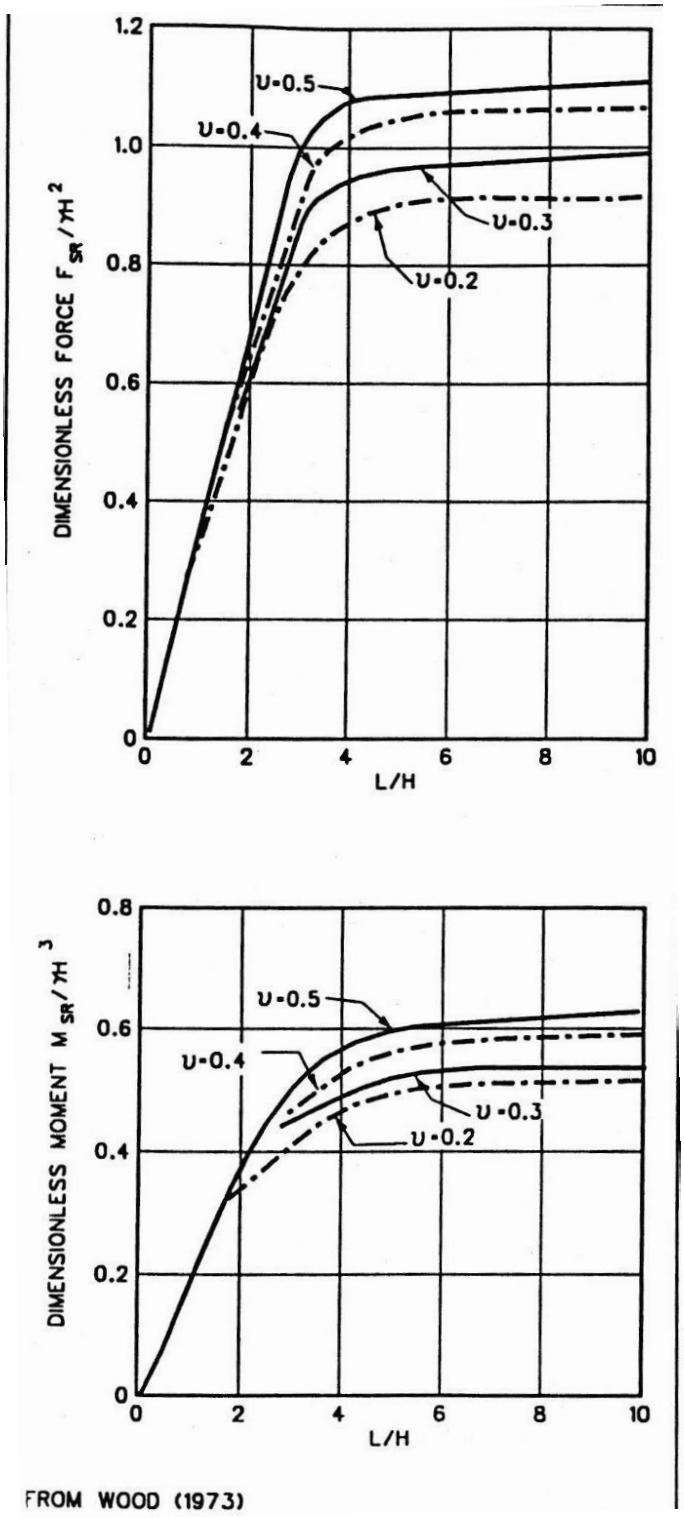

Figure E-7-12 – Forces and Moments from Wood's Solution (from Ebeling and Morrison, 1992)

E-7.3 Finite Element Model of Soil/Wall System

A possible alternative to the simplified approaches represented by the Mononobe-Okabe theory and Wood's solution is to construct a finite element model of the wall/backfill system and subject the system to earthquake ground motions, so that the soil-structure interaction can (in theory) be more accurately modeled. Keys to this time-history approach are to model the soil with non-linear soil properties so that the soil can yield and to model appropriate contact surfaces between the wall and the soil backfill. This approach was used at Pineview Dam and resulted in earth pressures that were between those predicted by the Mononobe-Okabe theory and Wood's solution. Research is currently in progress at Reclamation to develop procedures for evaluating soil-structure interaction, using both LS-DYNA and FLAC numerical codes. The finite element model for the Bradbury Dam spillway, which incorporates the entire embankment dam, is shown in Figures E-7-13 and E-7-14.

It should be noted that this approach is considerably more time-consuming and costly than the simplified approaches, and currently should only be considered for critical cases where the geometry is considerably different than that represented by the simplified methods, or the simplified linear-elastic methods show a wall is likely to fail producing high risks and a more detailed evaluation is desired before initiating corrective action. Since nonlinear modeling is needed, a significant amount of effort is needed to verify and test the model. Small changes in boundary conditions, the way the load is applied, or other modeling parameters can significantly change the results. Sensitivity analyses are critical when performing these types of studies to evaluate non-linear changes in soil properties, boundary conditions and methods of applying loads. Models also need to be verified which includes confirming that active, passive or at-rest static earth pressures can be achieved and that the interaction between the wall and soil backfill during shaking is reasonable.

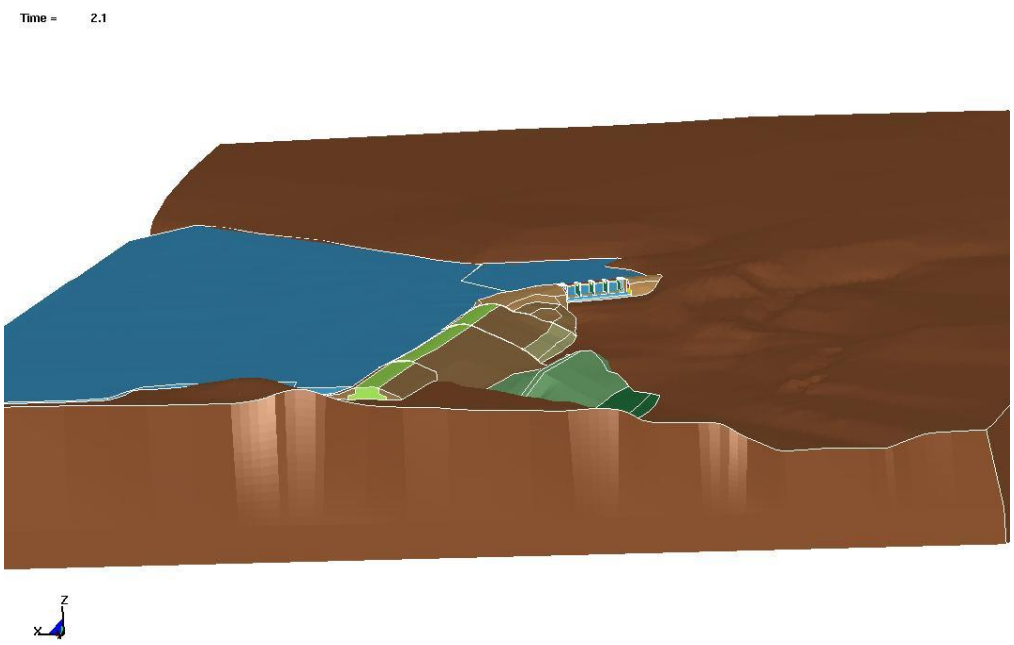

Figure E-7-13 – Bradbury Dam Spillway Finite Element Model

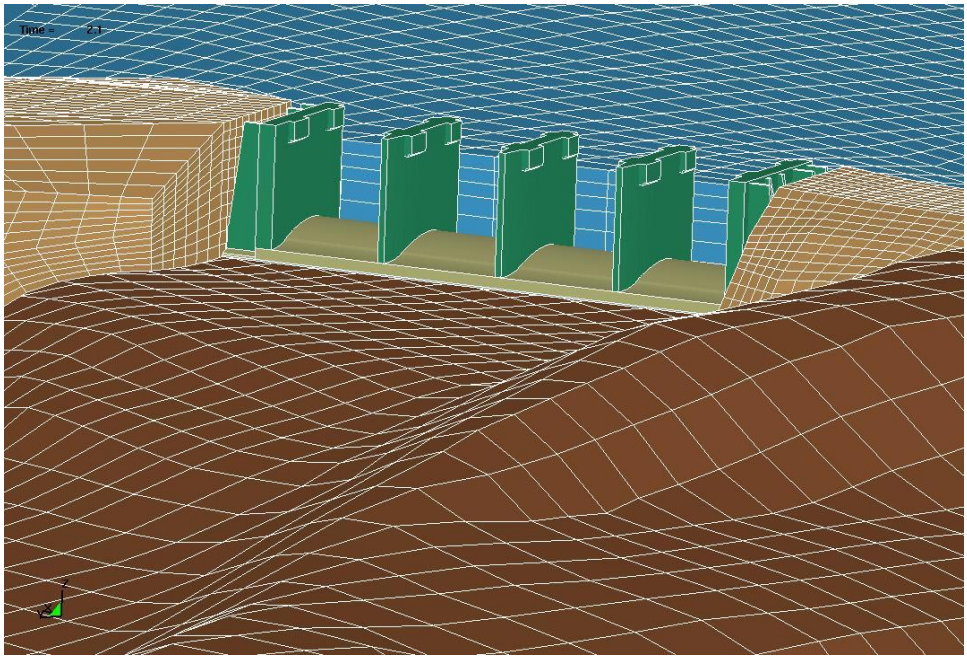

Figure E-7-14 – Close-up of Spillway in Bradbury Dam Finite Element Model

A promising development in the analysis of spillway crest structure walls is the modeling of reinforced concrete with non-linear material properties. Modeling the non-linear behavior of the concrete provides a method to evaluate the extents of concrete cracking and reinforcement yielding under seismic loading conditions and provides better insight into how loads might be redistributed within the structure once localized damage occurs. These detailed, non-linear finite element models tend to indicate that these structure have greater capacities than originally assumed or predicted by linear methods of analysis. An example of such a non-linear model is shown in Figure E-7-15 that show a non-linear finite element model of the crest structure at Scoggins Dam. The graphical output for these models illustrates expected cracking patterns as shown on Figure E-7-15. These cracking patterns along with reinforcement yielding information provides a much clearer picture for the risk analysis team regarding the extent of damage expected during the earthquake and the potential failure mechanism for the wall.

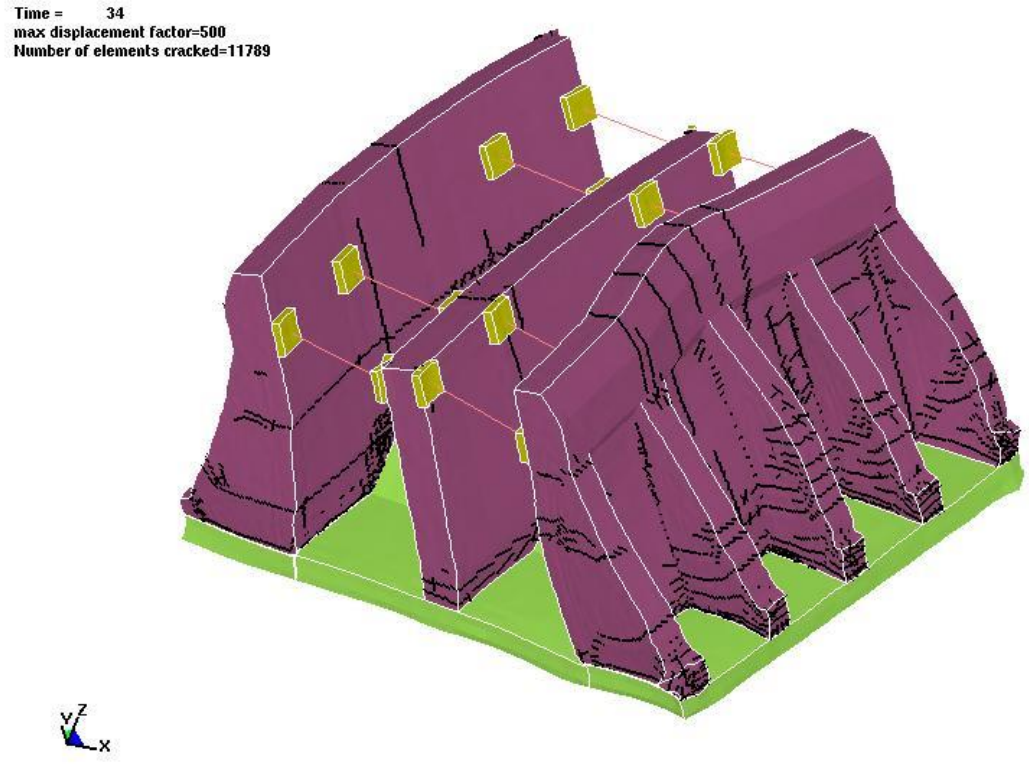

Figure E-7-15 – Non-linear Finite Element Model Results Showing Expected Cracking Patterns Resulting from Earthquake Loads

E-7.4 Centrifuge Modeling of Retaining Walls

Recent centrifuge modeling of retaining walls has been conducted at the University of California Davis, with the focus on seismic earth pressures (Sitar and Al-Atik, 2009). Two different walls were tested in the centrifuge runs – a flexible wall and a stiffer wall. The U-shaped retaining wall structures were placed side by side in the model container with soil placed underneath and behind each of the walls that form the U-shaped retaining structure as shown in Figure E-7-16. Multiple sets of instrumentation were installed to monitor the loadings on the wall. Flexiforce sensors were used to measure lateral earth pressures on the walls. Strain gages were used to determine bending moments in the wall and this information was used to back calculate earth pressures on the walls. Direct measurements of total moments at the bases of the walls were made using force-sensing bolts.

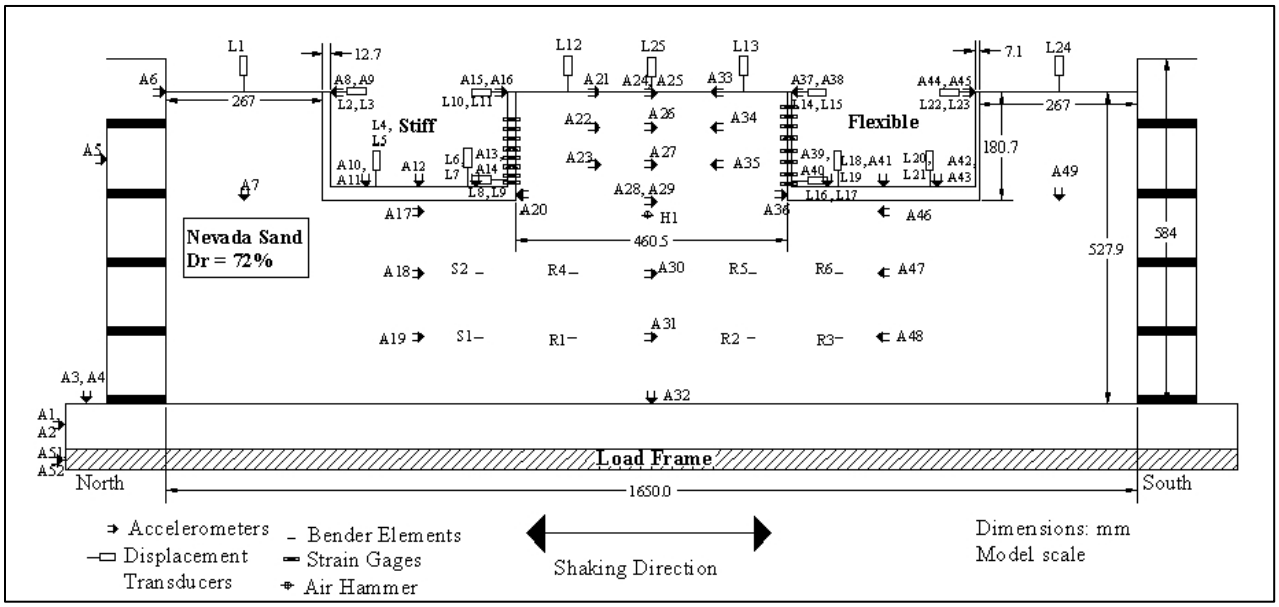

Figure E-7-16 – Centrifuge Model Test Setup

In addition to the centrifuge modeling, the research conducted by Sitar and Al-Atik included numerical modeling of the centrifuge models. The centrifuge model results were used to calibrate the soil model in the numerical code. In general, the same behavior was observed in the physical and numerical models.

Some of key findings from the research are as follows:

1. The wall inertial moments contribution to the overall dynamic wall moments is substantial and needs to be accounted for.
2. Wall inertial moments are generally in phase with the with dynamic wall moments.
3. Moments generated by the earth pressure on the wall are out of phase with the dynamic wall moments (at least for the test configuration).
4. The earth pressure distributions are triangular, increasing from no pressure at the top of backfill to maximum pressure at the base of the wall.
5. Earth pressures on the walls were less than those predicted by Mononobe-Okabe. The differences between the pressures measured from the experiments and those predicted by the Mononobe-Okabe method were reduced for the stiffer wall as compared to the more flexible wall.

Further research using similar centrifuge testing and numerical modeling has been conducted examining cohesive soils and cohesionless soils (Candia Agusti & Sitar, Geraili Mikola & Sitar). The results from Geraili Mikola and Sitar are comparable to some of the results obtained from finite element models of spillway crest structure walls founded on rock. The Geraili Mikola and Sitar results indicate that traditional methods (Mononobe-Okabe and Wood's) may overestimate seismic earth pressures, and recent finite element model study results have estimated earth pressures that are more in keeping with the findings of Geraili Mikola and Sitar than with traditional methods.

E-7.5 Structural Analysis

Simplified methods for estimating the moments and shears in a member during seismic loading include the use of the Mononobe-Okabe method (for active earth pressure conditions) or Wood's solution (for a stiff wall with at-rest earth pressure conditions) to compute the seismic earth pressures acting on the wall during the earthquake. As discussed above, research is currently ongoing to determine if there are specific geometries where the results from the simplified methods are unconservative and higher loads than those predicted by the simplified analyses

could result. Until more definitive finite element results become available, it is generally assumed that if the simplified approaches indicate that the moments and shear stresses are below the moment and shear capacities, the results will generally be conclusive and the likelihood of failure is low. If the simplified analyses indicate wall failure is likely and subsequent risks are estimated to be high, then the only available option may be to conduct a comprehensive non-linear finite element analysis to reduce uncertainty associated with this potential failure mode.

E-7.6 Event Tree

Figure E-7-17 is an example of an event tree for this potential failure mode. The event tree consists of a number of events that lead from initiation, through progression, to breach of the reservoir through gates that are lost as a result of wall failure. It is also possible that a breach of an embankment dam could result from spillway wall failure, if the dam is adjacent to one of the spillway crest structure walls. This first node represents the starting reservoir water surface elevation and the second node represents seismic load ranges. The combination of these first two nodes represents the combined load probability and affects the loading on the walls in the cross-canyon direction. Generally, the cross-canyon direction seismic loading is the focus of this potential failure mode because of the magnitude of the loads generated by the seismic earth pressures acting on the walls.

The remaining nodes in the event tree represent the conditional failure probability given the load probability. They are patterned after the general event tree for failure of reinforced concrete members, as described in the section on Reinforced Concrete Failure Mechanisms. First the likelihood of the concrete cracking from internal tensile stresses that develop as a result of applied seismic loads. As part of this evaluation, the potential for crushing of the concrete is also checked. If the concrete is not expected to crack, the shear capacity of the intact wall is checked. If the shear capacity of the wall is exceeded, the potential kinematic instability of the wall resulting from inadequate shear capacity is evaluated to determine if the wall would slide or topple to the extent necessary to fail the adjacent spillway gates or create a seepage path between the back side of the wall and the backfill.

If the concrete is expected to crack, then the likelihood of the reinforcement yielding is evaluated. The likelihood of the reinforcement yielding is typically estimated based on the computed moments at a critical section of the wall (typically the base of the wall) and the estimated moment capacity of the member at that section. The reinforcement could remain elastic or yield, depending on the moment demand in comparison to the computed capacity. If the reinforcement remains elastic, then the likelihood of exceeding the shear capacity is again checked with the concrete cracked. If the shear capacity is exceeded then the kinematic instability of the wall is evaluated. If the reinforcement yields, then once again the likelihood for shear failure is estimated, this time with cracked concrete section and yielded reinforcement. If the shear capacity is exceeded then kinematic instability of the wall is checked. If the shear capacity is not exceeded, the likelihood of uncontrolled non-linear wall displacement leading to gate collapse is estimated. A final check is performed on the potential for a seepage path being created between the wall and the backfill (which could consist of the embankment dam). If a seepage path is created, an additional evaluation of internal erosion along the seepage path is needed. Additional details regarding key factors and considerations for each one of these nodes is provided in the section for Reinforced Concrete Failure Mechanisms.

The event tree for seismic failure of walls is very similar to the event tree in the Seismic Spillway Pier Failure section. One difference however, is that kinematic instability for this potential failure mode requires a more detailed evaluation of the post-seismic condition of the wall in terms of the ability of the damaged wall to carry the post-seismic lateral earth pressures. The reason for this is that the backfill will provide a constant load, even after the earthquake has ended that could lead to complete failure and collapse of the wall. Refer also to the section on Event Trees for other event tree considerations. With the tools available, the estimates for many nodes on the event tree must by necessity be subjective (see the section on Subjective Probability and Expert Elicitation).

If a counterforted wall is being evaluated, the analysis and possibly the risk analysis will be more complicated. The analysis should evaluate both failure of the counterforts and the wall panels between the counterforts. The more critical component of the structure should be evaluated in

the risk analysis. The potential lateral support provided by bridge members that span the spillway crest structure could also affect analysis results and the corresponding risk estimates as discussed on the section Seismic Spillway Pier Failure section.

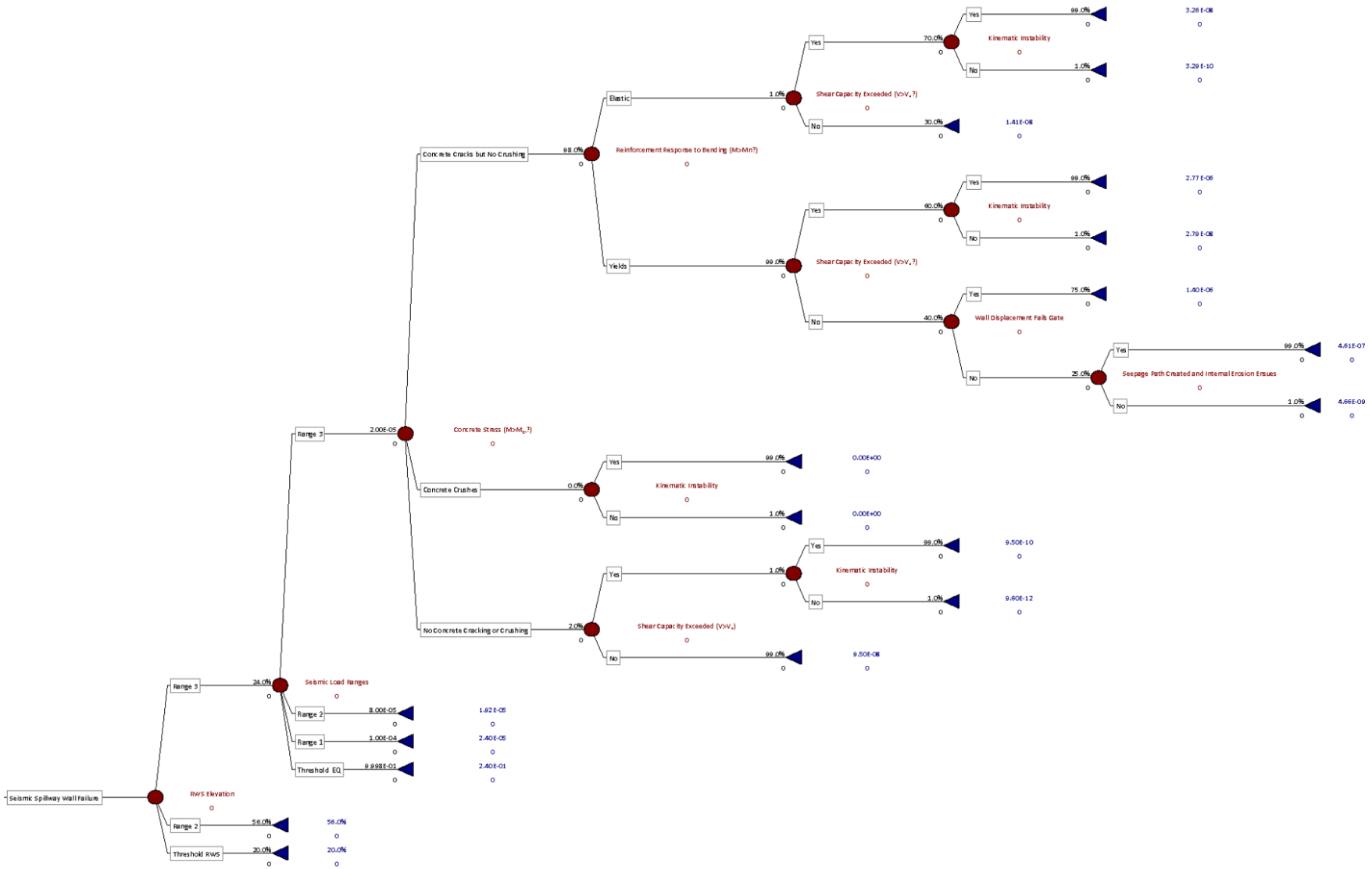

Figure E-7-17 – Example Event Tree for Seismic Spillway Wall Failure

E-7.7 Node 1 - Reservoir Water Surface Elevation

Reservoir load ranges are typically chosen to represent a reasonable breakdown of reservoir elevations from the normal water surface (i.e., maximum controllable reservoir water surface elevation that may be associated with the top of active conservation storage or the top of joint use storage) to an elevation within the lower half of the spillway walls, where there is a very small probability of an uncontrolled release. The number of load ranges depends on the variation in failure probability, and should be chosen, to the extent possible, to avoid large differences in failure probability at the top and bottom of the selected ranges. Historical reservoir elevation data can be used to generate the probability of the reservoir being within the chosen reservoir ranges, as described in the section on Reservoir (and River Stage) Exceedance Probabilities.

E-7.8 Node 2- Seismic Load Ranges

Seismic load ranges are typically chosen to provide a reasonable breakdown of the earthquake loads, again taking into account the variation in failure probability to avoid large differences between the top and bottom of each range. The total range should include loading from the threshold level at the lower end, to the level at which failure is nearly certain at the upper end. The total load range is generally subjective depending on the available seismic hazard curves and analysis information., . Seismic hazard curves are used to generate the probability distributions for the seismic load ranges as described in the section on Probabilistic Seismic Hazard Analysis.

It is preferable to identify appropriate load ranges, based on expected wall behavior from simplified analyses, prior to selecting the ground motions for FEM analysis and instead of selecting the ground motions based on recurrence intervals. For example, there may not be much difference between the results of analysis with the 10,000-year and 50,000-year earthquakes if both return periods have very high PHA. If those are what the structural analysts have been provided with, the risk-estimating team may find that it has no way to determine the likelihood of failure with smaller, more likely loadings. Therefore, it is important that the structural analysts meet with the seismologists before ground motion time histories are provided, so that the time histories cover the full range of motions for which the likelihood of wall failure is not trivial.

E-7.9 Node 3 – Concrete Stress

This node evaluates whether or not the tensile capacity of the concrete will be exceeded at the face of the wall and whether tensile cracking of the concrete will initiate. This can be determined by comparing calculated applied moments for the wall to the cracking moment of the section under investigation. If the cracking moment is exceeded, cracking will occur. The following equation can be used to calculate the cracking moment:

$M_{cr} = f_r I_g / y_{t,}$, **Equation E-7-9**

where f_r = concrete tensile strength

I_g = moment of inertia of the gross concrete section

y_t = distance from the centroidal axis of gross concrete section to the extreme tension fiber

Another approach is to compare tensile stresses in the wall to the tensile strength of the wall concrete. If test data are available, this information should be used to determine the tensile strength of the wall concrete. In the absence of actual data, the tensile strength of concrete can be determined using the considerations discussed in the section on Concrete Gravity Dams and Concrete Material Properties. If a finite element analysis has been performed, the tensile stresses computed at the faces of the wall can be compared directly to an estimated tensile strength value to evaluate this node. If a time history analysis is performed, the number of excursions in which the tensile stresses exceed the tensile strength of the concrete can be determined. If many excursions occur, it is very likely the wall section will crack through its entire thickness. If one or two isolated excursions occur, a less likely estimate for this node will be justified. The lateral extent over which cracking is predicted to occur is also important in terms of evaluating the remaining nodes of the event tree.

There is the potential for large compressive stresses to cause crushing of the wall concrete and this is checked as part of this node. Reclamation structures, including the walls, are typically massive and under reinforced, so concrete crushing is not a common issue.

E-7.10 Node 4 - Reinforcement Response to Bending

If the cracking moment is exceeded, this node evaluates the likelihood of the reinforcement yielding for each earthquake load range.

This node is evaluated by comparing the moments calculated from the earthquake (typically in the cross-canyon direction) to the expected moment capacity of the wall when the reinforcing steel reaches its yield value. If a time history analysis is performed, the moment demand-capacity ratio can be calculated at time steps during an earthquake. Axial tension resulting from vertical components of the earthquake or from vertical reaction components from the radial gates should also be considered. The number of excursions when the demand-capacity exceeds 1.0 and the extent to which it is exceeded are key factors for estimating this node of the event tree. A flexural yielding response curve for evaluating yielding of a reinforced concrete member is provided in the section on Reinforced Concrete Failure Mechanisms.

If moments during the earthquake are less than the yield moment capacity of the wall, then the section under investigation is generally considered to remain elastic during the earthquake.

E-7.11 Node 5 - Shear Capacity Exceeded

This node includes evaluation of the shear capacity of the wall in the context of three potential member conditions based on the outcomes of preceding nodes. Specifically, at this node the condition of the wall is one of the three options below:

1. Uncracked and has demonstrated the ability to carry applied moments based on the expected concrete tensile strength as if the section were unreinforced,
2. Cracked but with reinforcement carrying applied moments and forces within the expected elastic (unyielded) capacity of the section, or
3. Cracked with reinforcement that has yielded resulting in the onset of non-linear behavior of the member.

Regardless of which of the three states the wall is in at this node, the shear stresses during the earthquake are compared to the expected shear capacity of the wall based on its damaged state, if

applicable. As an example, if a construction joint exists within the spillway wall that is not fully bonded, this will create a weak plane in the wall through which a shear failure can occur. In this case, the failure location and the shear capacity should be adjusted accordingly. Additionally, if the trunnion anchorage for the spillway gates is located above a critical construction joint (that is at least partially unbonded), the total load resisted by the anchorage will have to be carried across the construction joint. If the shear capacity is exceeded, failure of the spillway wall and subsequent failure of the spillway gates is possible. Similarly, if the reinforcement for the section under investigation has yielded, the likelihood that the reinforcement at that section would also provide some additional shear capacity in the form of shear friction reinforcement would be considered less likely than for an elastic section.

Regardless of the damaged condition of the section, if the shear capacity is exceeded, a brittle failure of the wall may occur, with little to no chance of intervention. A discussion regarding various methods for estimating shear capacity of reinforced concrete members and an example shear response curve for evaluating shear failure of a reinforced concrete member for various demand capacity ratios is provided in the section on Reinforced Concrete Failure Mechanisms.

E-7.12 Node 6 - Wall Displacement Fails Gate

Even if a spillway wall does not fail catastrophically in shear, once the reinforcement yields, the wall may deflect enough to laterally load a spillway gate and cause the spillway gate to fail. For radial gates, a certain amount of deflection will be required to load the main horizontal structural elements of the gate. The gate seals and the outer edge of the skinplate provide some room for deflections to occur without impacting horizontal beams. As discussed in the Section on Reinforced Concrete Failure Mechanisms, the extent to which the wall may deflect before uncontrolled non-linear displacement occurs can be evaluated by using displacement criteria (Gulkan and Sozen, 1974; Otani and Sozen, 1974), which indicates that reinforced concrete structures can achieve 2 to 3 times the yield displacement of the structure and still be capable of supporting applied loads. If the calculated displacements exceed 2 to 3 times the yield displacement, the wall would likely topple or the gates would likely be subjected to the full weight of the walls.

E-7.13 Node 7 - Kinematic Instability

This node evaluates the kinematic instability of the damaged member. Specifically, at this node in the event tree the member under investigation is either inadequate to carry applied seismic loads in shear or has yielded to the extent necessary that significant non-linear displacements have occurred. If the shear capacity is exceeded the wall can become unstable as a result of earthquake loading due to either sliding or toppling depending on the geometry of the wall and the locations of the more severely damaged sections. If deflection criteria is exceed the wall may topple during the earthquake, but could slide post-seismically under sustained (static) loads imposed by the backfill due to the reduced shear capacity of the damaged section. However, it is also possible that stability of the wall could be maintained such that the adjacent gates do not fail, particularly for walls that are braced at the top. Additionally, in general, walls with a larger base to height ratio will be more stable than walls with a smaller base to height ratio.

E-7.14 Node 8 - Wall Deflection Creates Seepage Path between Embankment and Wall and Internal Erosion Ensues

If a spillway wall does not fail in shear and regardless of whether the wall deflects to the extent necessary to fail the spillway gates, the wall may still deflect enough to create a separation and potential seepage path between the wall and the adjacent fill material. This is most critical for spillways adjacent to embankment dams, where the embankment serves as backfill for one of the crest structure walls. Erosion of the embankment materials has the potential to result in a breach of the embankment and a subsequent large breach outflow.

The creation of the seepage path will be a function of the amount of wall deflection and the properties of the backfill soil. If the backfill or portions of the backfill are cohesionless, the fill may be able to adapt and move with the wall during an earthquake, preventing a separation between the wall and the backfill. If the backfill material has more plasticity, it is more likely that wall deflection will create a gap and prevent the backfill from moving with the wall and filling in any gaps that are created. If a potential seepage path is created that flows can enter and exit and if the reservoir level is high enough to access the seepage path behind the wall, erosion of the backfill may initiate and progress to dam breach. Evaluation of this node typically

requires development of a separate internal erosion event tree, as described in the section on Seismic Risks for Embankments.

E-7.15 Consequences

Consequences will be a function of the extent of the wall failure. A breach outflow that results from gate failure as a result of wall deflections will typically be limited to the outflow from one or two outside gates of the spillway crest structure and will be a function of the reservoir elevation at the time of gate failure. A much larger breach outflow could result if the dam embankment is placed directly against one of the walls and an erosional breach of the dam occurs.

The breach of the embankment can occur from several scenarios. One scenario is that the spillway crest structure wall adjacent to the embankment fails catastrophically and the spillway gate adjacent to the failed wall also collapses. If the reservoir is above the spillway crest elevation, the embankment adjacent to the wall will be directly exposed to flow through the damaged spillway bay, likely resulting in lateral erosion of the embankment and a breach of the dam. The second scenario for dam breach will be a case where the wall fails by deflecting excessively but does not impact the adjacent gate and still retains its structural integrity during and after the earthquake. The deflections of the walls could create a seepage path behind the wall. If the reservoir level is high enough to access the seepage path created behind the wall internal erosion can initiate, progress, and lead to breach of the dam. The extent of the dam breach will be a function of the embankment geometry and materials, the embankment foundation materials, and the location of the spillway relative to the embankment.

E-7.16 Results

The complete event tree described for this potential failure mode will have many branches. Due to the large number of load ranges, it may be easier to enter the event tree as rows and columns in a spreadsheet than to use Precision Tree. If Precision Tree is used, the resulting tree will likely take up several pages. It is important to review the results and isolate the major risk contributors.

E-7.17 Accounting for Uncertainty

The method of accounting for uncertainty in the seismic loading is described in the sections on Probabilistic Seismic Hazard Analysis. Typically, the reservoir elevation exceedance probabilities are taken directly from the historical reservoir operations data, which do not account for uncertainty. Uncertainty in the failure probability and consequences are accounted for by entering the estimates as distributions rather than single point values. A "Monte-Carlo" simulation is then run to display the uncertainty in the estimates, as described in the section on Combining and Portraying Risks.

E-7.18 Relevant Case Histories

There are limited cases of failure of spillway walls during earthquakes, and generally retaining walls have performed well during seismic loading. Despite this, the potential for this potential failure mode exists and is possible given a critical combination of earthquake loading, reservoir loading and the resulting stresses in the spillway walls.

E-7.18.1 Austrian Dam, California

Austrian Dam is a 200-foot high embankment dam that was constructed in 1949 to 1950 and is located on Los Gatos Creek, near the town of Los Gatos, California. A concrete spillway is located on the right abutment of the dam. The uncontrolled ogee crest structure is founded on moderately weathered fractured shale and the crest elevation is 15 feet below the dam crest elevation. The spillway chute is founded on highly weathered shale, but some of the shale was replaced with shallow compacted fill during construction. Austrian Dam was subjected to the Loma Prieta earthquake on October 17, 1989. The earthquake was a magnitude 7.1 event and was centered in the Southern Santa Cruz mountains, near the Loma Prieta Lookout. It is estimated that the peak horizontal ground accelerations at Austrian Dam were up to 0.6g.

Austrian Dam settled and spread in the upstream and downstream directions as a result of the earthquake. The maximum settlement of the dam was 2.8 feet; maximum downstream movement near the spillway wall on the right abutment was 1.1 feet; and, the maximum upstream movement was 1.4 feet, near the left quarter point of the embankment. Longitudinal cracks up to 14 feet deep occurred within the upper portions of the upstream and downstream

faces of the dam. Transverse cracking (to a depth of 32 feet on the right abutment) and embankment separation from the spillway structure occurred (USCOLD, 1992).

The spillway was damaged as a result of the earthquake loading. Cutoff walls were provided along the length of the spillway walls and the cutoffs were loaded and displaced as the embankment spread in the downstream direction. The spillway structure elongated about one foot as a result of the embankment deformation as shown in Figure E-7-18. Voids up to 6 inches were created upstream of the cutoff walls. The walls of the "U" shaped chute deflected inward, which lifted the base of the structure and the adjacent portions of the chute floor slab up to 1 inch. While the spillway did not fail catastrophically, the structure was severely damaged and a potential seepage path was created along the left spillway wall, due to the separation of the wall and the adjacent embankment. Fortunately, the reservoir was low at the time of the earthquake.

Figure E-7-18 – Elongated Spillway Wall at Austrian Dam

E-7.18.2 Shi-Kang Dam, Taiwan

Shi-Kang Dam is a buttress gravity dam located on the Tachia River. The dam is located about 50 km north of epicenter of the Chi-Chi earthquake, which occurred on September 21, 1999. The Chelungpu fault passed underneath the spillway crest structure and ruptured during the Chi-Chi earthquake. Differential movement along the (spillway bays 16 to 18) fault was about 29 feet in the vertical direction and 6.5 feet in the horizontal direction. Peak ground acceleration was reported at 0.56g in a town near the dam, but there was evidence that ground motions at the site were not that intense. The spillway bays outside of bays 16 to 18 survived with little or no damage (USCOLD, 2000).

Figure E-7-19 shows the failure of a chute wall panel in the spillway for Shi-Kang Dam. The wall is counterforted and it appears that the collapse of the wall resulted from a shear failure in the counterforts. No specific details are available regarding the failure but the failure demonstrates for the potential failure of spillway walls during large earthquakes.

Figure E-7-19 – Failed Spillway Wall at Shih-Kang Dam

E-7.19 Considerations for Comprehensive Review/Periodic Assessment

The complete analysis as described in this section is likely to be too time consuming to be performed during a Comprehensive Review (CR) or a Periodic Assessment (PA). Therefore, simplifications must be made. Fewer load ranges are typically evaluated and only the expected value estimates are entered into the event tree. A simple pseudo-static seismic analysis of a spillway wall can be performed if analysis results do not exist. Seismic earth pressures can be calculated using either Mononobe-Okabe or Wood's equations. Based on the loads described above, the moments and shears can be calculated at various elevations within the wall and compared to the moment and shear capacities at these locations.

E-7.20 Exercise

Consider a spillway with crest structure cantilever walls that are 2-feet thick at the base and 40-feet high. Calculate the shear stresses at the base of the wall for the earthquakes described in Table E-7-2, using Mononobe-Okabe for active earth pressures and assuming cohesionless backfill with a friction angle of 30° and a density of 120 lb/ft^3. Assume that the backfill is at the top of the walls and that the backfill surface is horizontal. Assume that the angle of interface friction (δ) is 15°. Assume that the shear capacity of the spillway walls is 200 lb/in^2, and that it remains constant for all loading conditions. Based on a comparison of the shear stress at the base of the wall to the shear capacity of the wall concrete, estimate the probability that the shear capacity will be exceeded for the 1000-, 5000-, 10,000-, and 50,000-year earthquake. Assume that there is no vertical component of the ground motions.

Table E-7-2 – Spillway Wall Analysis – Earthquake Loads

Recurrence Interval, yr	Peak Horizontal Ground Acceleration
1000	0.1g
5,000	0.2g
10,000	0.3g
50,000	0.4g

E-7.21 References

American Concrete Institute, *Building Code Requirements for Structural Concrete (ACI 318-05) and Commentary (ACI-318R-05),* Reported by ACI Committee 318, , August 2005.

California Department of Transportation (Caltrans) "Memo to Designers 20-4, Attachment B," August 1996.

Candia Agusti, G., Sitar, N., "Seismic Earth Pressures on Retaining Structures in Cohesive Soils," Report submitted to the California Department of Transportation (Caltrans) under Contract No. 65A0367 and NSF-NEES-CR Grant No. CMMI-0936376: Seismic Earth Pressures on Retaining Structures, Report No. UCB GT 13-02, August 2013.

Clough, G.W. and Duncan, J.M., Chapter 6: Earth Pressures, in *Foundation Engineering Handbook,* Second Edition, edited by H.Y. Fang, Von Nostrand Reinhold, NY, 1991.

Duncan, J.M., Williams, G.W., Sehn, A.L, and Seed, R.B., "Estimation of Earth Pressures Due to Compaction," Journal of Geotechnical Engineering, Vol. 117, No. 12, December 1991.

Ebeling, Robert M., and Morrison, Ernest E., *The Seismic Design of Waterfront Retaining Structures, U.S. Army, Technical Report ITL-92-11, U.S. Navy, Technical Report NCEL TR-939,* Department of the Army, Waterways Experiment Station, Corps of Engineers, November 1992.

Geraili Mikola, R., and Sitar, N., "Seismic Earth Pressures on Retaining Structures in Cohesionless Soils," Report submitted to the California Department of Transportation (Caltrans) under Contract No. 65A0367 and NSF-NEES-CR Grant No. CMMI-0936376: Seismic Earth Pressures on Retaining Structures, Report No. UCB GT 13-01, March 2013.

Gulkan, P. and Sozen, M., "Inelastic Responses of Reinforced Concrete Structures to Earthquake Motions," ACI Journal, December 1974.

Matsuzawa H., Ishibashi I., and Kawamura, M., "Generalized Apparent Seismic Coefficient for Dynamic Lateral Earth Pressure Determination," Proceedings of 2nd International Conference on Soil Dynamics and Earthquake Engineering, edited by C. Brebbia, A. Cakmak, and A. Ghaffer, 1985.

Maleki, S., Mahjoubi, S., "A New Approach for Estimating the Seismic Soil Pressures on Retaining Walls," Transaction A: Civil Engineering, Vol. 17, No. 4, pp. 273-284, Sharif University of Technology, Iran, August, 2010.

Mononobe, N., and Matsuo, H., "On the Determination of Earth Pressures During Earthquakes," Proceedings, World Engineering Congress, 1929.

Okabe, S., "General Theory of Earth Pressure," Journal Japan Society of Civil Engineering, Vol. 12, No. 1, 1926.

Ostadan, F., White, W.H., "Lateral Seismic Soil Pressure – An Updated Approch," Bechtel Technical Grant Report, Bechtel Corporation, San Francisco, Calirfornia, 1997.

Otani, S. and Sozen, M., "Simulated Earthquake Tests of R/C Frames," Journal of the Structural Division, ASCE, March 1974.

Raphael, Jerome, M., "Tensile Strength of Concrete," American Concrete Institute, Technical Paper, Title No. 81-17, March-April, 1984.

Sitar, N. and Al-Atik, L., "On Seismic Response of Retaining Structures," Proceedings of International Conference on Performance Based Design in Earthquake Geotechnical Engineering, Tsukuba City, Japan, June 15-18, 2009.

Sherif, M. and Fang, Y., "Dynamic Earth Pressures Against Rotating and Non-Yielding Retaining Walls," Soil Engineering Research Report No. 23, Department of Civil Engineering, University of Washington, Seattle, Washington, November 1983.

United States Committee on Large Dams (USCOLD), "Observed Performance of Dams During Earthquakes," July 1992.

United States Committee on Large Dams, "Observed Performance of Dams During Earthquakes, Volume II," October 2000.

Whitman, J. and Christian, J., "Seismic Response of Retaining Structures," Symposium on Seismic Design for World Port 2020, Port of Los Angeles, Los Angeles, California, 1990.

Wood, J., "Earthquake-Induced Soil Pressures on Structures, Report No. EERL 73-05," California Institute of Technology, Pasadena, CA, 1973.

Wu, T.H., *Foundation Engineering Handbook*, Chapter 12 – Retaining Walls, Van Nostrand Reinhold Company, New York, 1975.

Yong, P.M.F., "Dynamic Earth Pressure Against A Rigid Earth Retaining Wall, Central Laboratories Report 5-8515, Ministry of Works and Development, Lower Hutt, New Zealand, 1985.